Dermal thirdhand smoke exposure induces oxidative damage, initiates skin inflammatory markers, and adversely alters the human plasma proteome

Shane Sakamaki-Ching,[a] Suzaynn Schick,[b] Gabriela Grigorean,[c] Jun Li,[d] and Prue Talbot[a]*

[a]Department of Molecular, Cell, and Systems Biology, University of California, Riverside, United States
[b]Center for Tobacco Control Research and Education, University of California, San Francisco, United States
[c]Proteomics Core Facility, University of California, Davis, United States
[d]Department of Statistics, University of California, Riverside, United States

Summary

Background Thirdhand smoke (THS) exposure correlated with significant metabolism of carcinogenic chemicals and the potential to cause detrimental health effects. Human harm research of THS exposure is limited to one other study and overall, there is a general lack of knowledge of the human health responses to THS exposure.

Methods This was a clinical investigation to evaluate the health effects of 3-h dermal THS exposure from urine and plasma. 10 healthy, non-smoking subjects were recruited for dermal exposure for 3 h exposed to clothing impregnated with filtered clean air or THS. Exposures to clean air or THS occurred 20-30 days apart.

Findings In THS-exposed group, there was a significant elevation of urinary 8-OHdG, 8-isoprostane, protein carbonyls. The THS 3-h exposure identified proteomics pathways of inflammatory response ($p=2.18 \times 10^{-8}$), adhesion of blood cells ($p=2.23 \times 10^{-8}$), atherosclerosis ($p=2.78 \times 10^{-9}$), and lichen planus ($p=1.77 \times 10^{-8}$). Nine canonical pathways were significantly activated including leukocyte extravasation signaling (z-score=3.0), and production of nitric oxide and reactive oxygen in macrophages (z-score=2.1). The THS 22-h proteomics pathways revealed inflammation of organ ($p=3.09 \times 10^{-8}$), keratinization of the epidermis ($p=4.0 \times 10^{-7}$), plaque psoriasis ($p=5.31 \times 10^{-7}$), and dermatitis ($p=6.0 \times 10^{-7}$). Two activated canonical pathways were production of nitric oxide and reactive oxygen in macrophages (z-score=2.646), and IL-8 signaling (z-score=2.0).

Interpretation This is a clinical study demonstrating that acute dermal exposure to THS mimics the harmful effects of cigarette smoking, alters the human plasma proteome, initiates mechanisms of skin inflammatory disease, and elevates urinary biomarkers of oxidative harm.

Funding Funding was provided by the Tobacco Related Disease Research Program (TRDRP) 24RT-0037 TRDRP, 24RT-0039 TRDRP, and 28PT-0081 TRDRP.

Keywords: Thirdhand smoke; Biomarkers; Proteomics; Oxidative stress; Inflammation; Skin disease

eBioMedicine 2022;84: 104256
Published online xxx
https://doi.org/10.1016/j.ebiom.2022.104256

Introduction

Thirdhand smoke (THS) is comprised of the residual tobacco smoke pollutants that remain on surfaces and in dust after tobacco has been smoked; are re-emitted into the gas phase; or react with oxidants and other compounds in the environment to yield secondary pollutants.[1] Some THS chemicals, including nicotine, react with environmental oxidants and produce secondary pollutants, such as tobacco-specific nitrosamines, that are harmful.[2,3] THS can remain on indoor surfaces indefinitely causing potentially harmful exposure to both smokers and non-smokers.[4,5]

In-vitro studies have demonstrated numerous harmful effects of THS exposure, including stress-induced mitochondrial hyperfusion and altered mitochondrial gene expression in mouse neural stem cells and human

*Corresponding author at: Department of Cell Biology & Neuroscience, University of California, Riverside, CA 92521, United States.
E-mail address: talbot@ucr.edu (P. Talbot).
The corresponding author attests that all listed authors meet authorship criteria and that no others meeting the criteria have been omitted.

Research in context

Evidence before this study

We searched PubMed, Google Scholar, and Thirdhand Smoke Research Consortium for all studies with the keywords "thirdhand smoke", "human", "human harm", "clinical trial", "clinical study", "biomarkers", "omics", and "skin". Only one study appeared which was a previous clinical study published from our lab of humans nasally exposed to inhaled THS. There is not a single clinical study of direct dermal THS exposure in humans that studied urinary biomarkers of harm and plasma proteomics.

Added value of this study

This is a clinical study that identified the molecular adverse health effects of THS dermal exposure in humans. These results provide urinary biomarkers and plasma proteomics pathway analysis of the effects of THS. These results demonstrate acute dermal THS exposure is not only harmful to humans, but also has the potential to initiate diseases.

Implications of all the available evidence

These results will aid physicians in the diagnosis of patients exposed to THS and guide future research in the molecular mechanisms of THS toxicity. Our study aids in the molecular understanding of the effects of THS on the skin and may aid in the development of regulatory policies dealing with remediation of indoor environments contaminated with THS.

embryonic stem cells.[6] Cytotoxicity of THS in the MTT assay was attributable to acrolein.[7] THS also produced DNA strand breaks in human liver (HepG2)[8] and caused metabolomic changes consistent with an antioxidant response in male reproductive cells.[9] Mice exposed to THS fabric in their cages had increased liver lipids and non-alcoholic fatty liver disease, excess collagen and increased inflammatory cytokines in their lungs, and decreased wound healing capacity.[10] THS-exposed mice showed increased platelet aggregation and hyperactivity, which increased the risk for thrombosis.[11] A 4-week THS-exposure in mice increased the risk of lung cancer incidence,[12] and another mouse metabolomics study showed liver damage attributed to oxidative stress.[13]

Clinical research on harm caused by THS is limited to two studies. One study evaluated the relationship between THS exposure of people living in homes of smokers and the risk of cancer. They measured nitrosamines in house dust, estimated a lifetime exposure, and found a greater cancer risk if people were exposed at a young age.[14] A second study analysed gene expression in nasal epithelium following acute inhalation of THS emitted from a controlled chamber. Affected genes were associated with increased mitochondrial activity, oxidative stress, DNA repair, cell survival, and inhibition of cell death,[15] showing that humans respond to inhaled THS chemicals. However, no studies have been done on humans exposed dermally.

The three main routes of THS exposure are inhalation, ingestion, and dermal. Skin is the largest organ to contact THS and may receive the greatest exposure. The purpose of our crossover clinical investigation was to assess the potential health effects of dermal exposure to THS by measuring biomarkers of oxidative stress in urine and plasma and changes in the plasma proteome. Ten healthy, adult nonsmokers wore clothing impregnated with THS for 3 h with 15 min of exercise in each hour to induce perspiration. Control exposure participants wore clean clothing for the same time with the same exercise. Urine samples collected before exposure, immediately after exposure (3 h), at 8 h, the next morning, and 22 h after exposure were analysed for biomarkers of exposure and harm, and the plasma proteome was analysed to identify effects on protein expression.

Methods

Study protocol and ethics

The study CONSORT diagram describes the protocol, participant's exposure, and sample collection (Figure 1). The study was approved with patient informed consent by the human research protection program Institutional Review Board (IRB#15-17009) by the San Francisco General Hospital Panel. Participant demographics (See Supplementary 1 Table 1), participant inclusion and exclusion criteria (See Supplementary 2, Clinical Protocol and Statistical Analysis), and sample analysis workflow (See Supplementary 1 Figure 1) are provided.

Study interventions

Briefly, 10 healthy, non-smoking subjects participated in a cross-over, randomised, unblinded study wearing clothing with or without THS for 3 h in the Human Exposure Laboratory at the San Francisco General Hospital. To increase dermal uptake, all participants exercised on a treadmill for 15 min/h to induce perspiration. The order of the exposures was randomised and separated by 20-30 days. Each participant received both exposures. The protocol for generating the clothing was described previously.[16] Urine and plasma were collected before exposure (0 h) and at 3 and 8 h after the start of exposure, upon waking the next morning, and at 22 h after the start of exposure. Samples were centrifuged, aliquoted, stored at -80°C, and shipped frozen to UCR for analysis.

Urine samples from 0, 3, 8, and 22 h were analysed for biomarkers and a subset of plasma samples from 5 participants, collected at 0, 3, and 22 h, were analysed by proteomic methods.

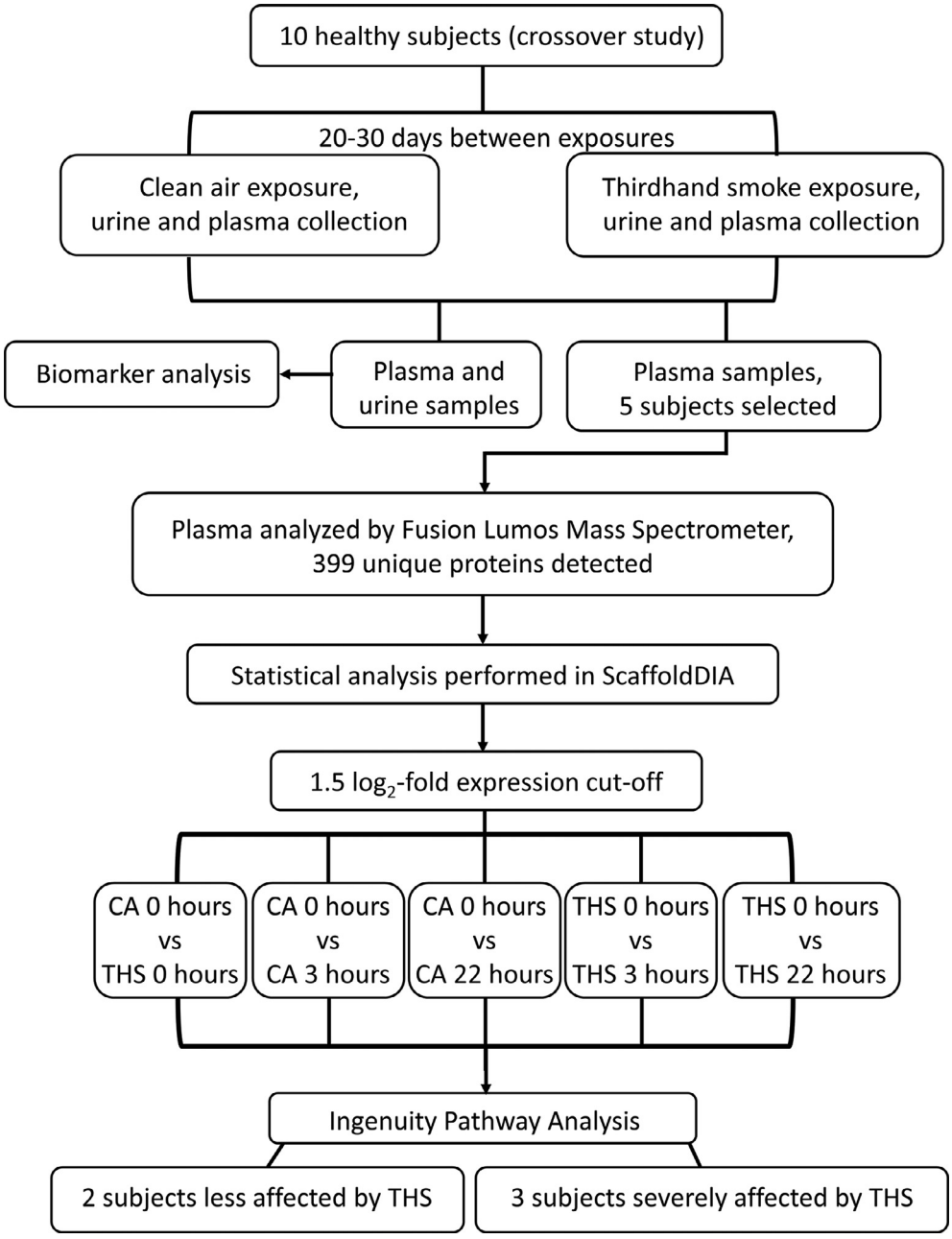

Figure 1. The study CONSORT diagram describes the protocol, participant's exposure, and sample collection. 10 healthy subjects were selected for a cross-over clean air or THS exposure for 3 h (exposures were separated 20-30 days apart). Urine and plasma were collected at pre-determined timepoints up to 22 h and analysed for urinary biomarkers of harm and global plasma proteomics. Proteomics results from the exposures were analysed for changes to canonical and disease pathways by IPA.

Sample size calculation

Sample size was determined based on the number of people sufficient to detect increases in markers of inflammation in previous studies of secondhand cigarette smoke exposure[17,18] (See Supplementary 2, Clinical Protocol and Statistical Analysis).

Data collection and statistical analysis

Urinary biomarker statistics. We conducted a repeated measures analysis using the mixed effects model in Prism 9.0 (GraphPad) because the urinary biomarker concentrations were collected over time from each

participant. There are two fixed factors in the mixed effects model we used: "time" (baseline, 3 h, 8 h, first morning or 22 h) and "treatment" (clear air or THS), and we have repeated measures in both factors. Before we carried out the repeated measures analysis in Prim 9.0 (GraphPad), we also applied the log transformation to the data in order for the assumptions of the mixed effects model we used to be met. After the repeated measures analysis using the mixed effects model was performed on the log-transformed data, we checked the significance of the factor "treatment" and it was found significant in all the urinary biomarkers (8-OHdG, 8-isoprostane and protein carbonyls). This indicates that the overall concentrations of the three urinary biomarkers over time are significantly different between clean air and THS. To find out at which time points the concentrations of the urinary biomarkers were significantly different between clean air and THS, we performed the following post-hoc multiple comparisons with Bonferroni correction in Prism 9.0 (GraphPad): clean air baseline vs THS baseline, clean air 3 h vs THS 3 h, clean air 8 h vs THS 8 h, clean air first morning vs THS first morning, and clean air 22 h vs THS 22 h. Results of those comparisons with Bonferroni adjusted p-values were reported in the Results Urinary Biomarkers of Potential Harm section. Biomarker graphs were made in Prism 9.0 (GraphPad). Significance is denotated as * $p \leq 0.05$, ** $p \leq 0.01$, *** $p \leq 0.001$.

Urinary biomarkers of potential harm. Urinary biomarkers were normalised to creatinine. 8-OHdG was measured using a DNA Damage ELISA Kit (SKT-120, Stress Marq Biosciences), following a 1:20 dilution. 8-isoprostane was measured following a 1:4 dilution using a Urinary 8-Isoprostane ELISA kit (8isoU1, Detroit R&D). Protein was quantified in 1:10 or 1:20 dilutions using the Pierce BCA Protein Assay Kit (23225, Thermofisher Scientific). Protein carbonyls were analysed using a Protein Carbonyl Assay Kit (ab126287, Abcam) protocol with reagents that were ordered separately. Total oxidized protein (nmol/ml) was normalised to the total protein concentration (mg/ml). Any datapoints that fell outside the limits-of-detection were removed from analysis. There was no effect due to gender or age.

Plasma proteomics sample preparation

The serum samples were solubilized in 50 µL of solubilization buffer and subjected to reduction/alkylation /tryptic proteolysis using suspension-trap (ProtiFi) devices. S-Trap is a powerful Filter-Aided Sample Preparation (FASP) method that traps acid aggregated proteins in a quartz filter prior to enzymatic proteolysis. Disulfide bonds were reduced with dithiothreitol and alkylated (in the dark) with iodoacetamide in 50 mM triethylammonium bicarbonate (TEAB) buffer. Digestion was done by addition of trypsin 1:100 enzyme: protein (wt/wt) for 4 h at 37°C, followed by a boost addition of trypsin using the same wt/wt ratios for overnight digestion at 37°C. Peptides, still in the S-Trap, were eluted using sequential elution buffers of 100 mM TEAB, 0.5% formic acid, and 50% acetonitrile 0.1% formic acid. The eluted tryptic peptides were dried in a vacuum centrifuge and re-constituted in 0.1% trifluoroacetic acid. The peptide extracts were reduced by vacuum centrifugation and a small portion of the extract was used for fluorometric peptide quantification (Thermo Scientific Pierce). One microgram of sample based on the fluorometric peptide assay was loaded for each LC-MS analysis.

Liquid chromatography tandem mass spectrometry

Peptides were desalted and trapped on a Thermo PepMap trap and separated on an Easy-spray 100 µm x 25 cm C18 column using a Dionex Ultimate 3000 RSLC at 200 nL/min. Solvent A = 0.1% formic acid, and solvent B = 100% acetonitrile 0.1% formic acid. Gradient conditions = 2% B to 50% B over 60 min, followed by a 50%−99% B in 6 min, then held for 3 min, then 99% B to 2% B in 2 min with a total run time of 90 min using a Thermo Scientific Fusion Lumos mass spectrometer. Two data acquisition modes were employed: data-dependent analysis DDA and data-independent analysis, DIA. The DDA mode was used to build spectral libraries, which were used to perform deep searches on the samples, run in DIA mode. To obtain the DDA runs, we pooled peptides from all our thirdhand smoke samples. Then, this pooled sample was divided, and eight DDA injections were performed. MS data for samples run in DIA mode cover the entire range of m/z 400−1200. Both DDA and DIA data were acquired using a collision energy of 35, resolution of 30 K, maximum inject time of 54 ms and a AGC target of 50 K, using staggered isolation windows of 12 Da.

Mass spectrometry data analysis

DIA data were analysed using Spectronaut (v.13, Biognosis) using the classic analysis DIA workflow with default settings. Prior to library-generation and analysis of the DIA LCMS runs, all raw files were converted into htrms files using the Htrms converter (Biognosys). MS1 and MS2 data were centroided during conversion, and the other parameters were set to default. A deep DDA spectral library was first generated by submitting the htrms files of the DDA gas-phase separation LCMS runs to a library generating step in Spectronaut. This uses the Pulsar search engine, and all DDA runs are searched against the Homo sapiens sequence database -Uniprot UP00005640. The DIA htrms files were submitted for identification/quantitative analysis to Spectronaut, using the previously generated deep DDA

spectral library (see above) and the reviewed Uniprot FASTA for Homo Sapiens, UP00005640. Default settings were used to perform this quantitative data analysis with the two libraries. Briefly, calibration was set to non-linear iRT calibration with precision the iRT selected. DIA data were matched against the above-described spectral library supplemented with decoys (library size fraction of 0.1), using dynamic mass tolerances.

Quantitative and statistical analyses were performed by processing protein peak areas determined by the Spectronaut software. The DIA data were processed for relative quantification comparing peptide peak areas from different conditions. For the DIA MS2 data sets, quantification was based on XICs of 3-6 MS/MS fragment ions, typically y- and b-ions, matching to specific peptides present in the spectral library. Interference correction was enabled on MS1 and MS2 levels. Precursor and protein identifications were filtered to 1% FDR, estimated using the mProphet algorithm, 74 and iRT profiling was enabled. Quantification was normalised to local the total ion chromatogram. Statistical comparison of relative protein changes was performed with paired t-tests. Finally, proteins identified with less than two unique peptides were excluded from the assay. The significance level was q-value less than 0.05%, and log2 ratio more than 0.58. Both DIA analysis results were filtered within Spectronaut by a 1% false discovery rate on the peptide and protein level using a target-decoy approach, which corresponds to a Q value <0.01.

Plasma proteomics analysis

Five subjects with increased urinary biomarkers of potential harm were selected for plasma proteomics, performed by a Fusion Lumos Mass Spectrometer (Invitrogen). Proteins were referenced by the PanHuman database containing 399 total proteins. Significantly expressed proteins were identified using a threshold cut-off of ± 1.5 $\log_2$ fold change and a 1% false detection rate. To determine significant protein expression between the clean air and THS groups at different timepoints, the subjects were compared as follows: baseline (clean air 0 h vs THS 0 h), clean air 3 h (clean 0 h vs clean air 3 h), clean air 22 h (clean air 0 h vs clean air 22 h), THS 3 h (THS 0 h vs THS 3 h), and THS 22 h (THS 0 h vs THS 22 h). The list of proteins analysed in each group are provided (See Supplementary 1 Table 2).

Biological processes, networks, and pathways were analysed using Gene Ontology (GO) and Ingenuity Pathway Analysis (IPA). In GO analysis, significant processes were identified by a $p \leq 0.05$, and in IPA significant pathways were identified with a z-score of ± 2.0 to indicate pathway direction. A principal component analysis suggested that two (361 and 366) of the five subjects were less responsive to THS exposure (See Supplementary 1 Figure 2). To gain a better understanding of the health of effects of THS, the three responsive subjects (234, 364, 370) were further analysed. Similar variations in response have been reported in proteomic studies of cancer biomarkers in cigarette smoker's plasma.[19]

Proteomics data sharing

All proteomics data was publicly available and uploaded to ftp://massive.ucsd.edu/MSV000089435/.

Participant and public involvement

No participants were involved in the design of the research or the outcome measures, nor were they involved in developmental plans for recruitment, implementation, or interpretation of the study. Participant were provided with informed consent prior to the start of the study.

Role of funder

The funder had no role in the study design, data collection, data analyses, interpretation, or writing of this report.

Results

Participants

This study was completed in 2018 when the target of 16 participants was met. Six subjects (37.5%) did not provide samples at all the timepoints or did not provide sufficient sample to complete all the experiments. The 10 (62.5%) remaining participants were selected for urinary biomarker analysis and were well matched in age and gender, and five (31.2%) participants were further analysed for plasma proteomics (See Supplementary 1 Table 1).

Primary outcomes

Urinary biomarkers of potential harm. 8-OHdG. Urinary 8-OHdG is a biomarker of DNA oxidation. There were no significant differences between 8-OHdG concentrations in the baseline THS group (100 ± 81.1 SD ng/mg) and clean air group (78.9 ± 48.0 SD ng/mg) ($p = 0.99$, mixed effects model), at the 8 h timepoint in the THS group (210.7 ± 242.2 SD ng/mg) and clean air group (135.6 ± 107.1 SD ng/mg) ($p=0.99$, mixed effects model), and neither the first morning timepoint in the THS group (196.6 ± 134.0 SD ng/mg) and clean air group (94.3 ± 66.6 SD ng/mg) ($p=0.36$, mixed effects model). At 3 h the THS group (223.1 ± 170.0 SD ng/mg) compared to the clean air group (86.1 ± 80.6 SD ng/mg) ($p = 0.02$, mixed effects model), and at 22 h the THS group (172.7 ± 175.9 SD ng/mg) compared to the clean air group (36.1 ± 17.4 SD ng/mg) ($p = 0.003$, mixed effects model) the concentrations of 8-OHdG were significant (Figure 2A).

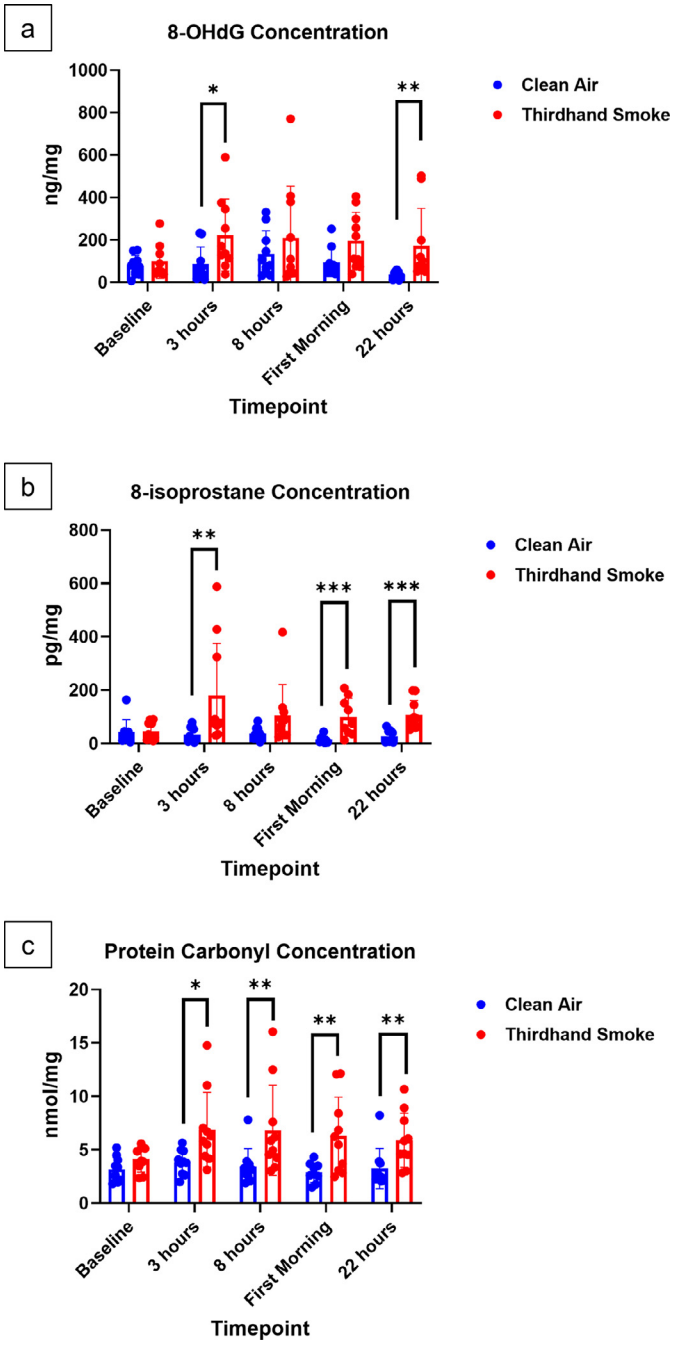

Figure 2. The THS-exposed subjects (n = 10) had significantly elevated urinary 8-OHdG, 8-isoprostane, and protein carbonyls compared to their clean air exposure timepoints. a. 8-OHdG concentrations (ng/mg of creatinine) at baseline, 3 h, 8 h, first morning collection, and 22 h, respectively. b. 8-isoprostane concentrations (pg/mg of creatinine) at baseline, 3 h, 8 h, first morning collection, and 22 h, respectively. c. Protein carbonyl concentrations (nmol/mg of creatinine) at baseline, 3 h, 8 h, first morning collection, and 22 h, respectively. The mean and standard deviation are reported. * $p \leq 0.05$, ** $p \leq 0.01$, *** $p \leq 0.001$ (mixed effects model).

8-Isoprostane. Urinary 8-isoprostane is a biomarker of lipid peroxidation. At baseline, there were no significant differences in 8-isoprostane concentrations between the THS group (45.6 ± 33.4 SD pg/mg) and the clean air group (42.3 ± 47.8 SD pg/mg) ($p = 0.99$, mixed effects model), and neither at the 8-h timepoint between the THS group (105.3 ± 115.7 SD ng/mg) and clean air group (37.4 ± 23.1 SD pg/mg) ($p = 0.12$, mixed effects

model). There were significant increases of 8-isoprostane concentration in the THS group compared to the clean air group at times: 3 h in the THS group (179.7 ± 195.5 SD ng/mg) and clean air group (34.5 ± 27.7 SD ng/mg) (p = 0.001, mixed effects model), first morning in the THS group (99.1 ± 70.3 SD ng/mg) and clean air group (14.7 ± 13.3 SD ng/mg) (p = 0.0002, mixed effects model), and 22 h in the THS group (106.9 ± 55.0 SD ng/mg) and clean air group (26.2 ± 23.5 SD ng/mg) (p = 0.0003, mixed effects model) (Figure 2B).

Protein carbonyl. Urinary protein carbonyl is a biomarker of protein oxidation. There were no significant differences in protein carbonyl concentration at baseline between the THS group (4.1 ± 1.2 SD nmol/mg) and the clean air group (3.2 ± 1.1 SD nmol/mg) (p = 0.64, mixed effects model). In contrast, there were significant increases in protein carbonyls at 3 h between the THS group (6.9 ± 3.5 SD nmol/mg) and clean air group (3.8 ± 1.1 SD nmol/mg) (p = 0.02, mixed effects model), at 8 h between the THS group (6.9 ± 4.2 SD nmol/mg) and clean air group (3.4 ± 1.7 SD nmol/mg) (p = 0.006, mixed effects model), in the first morning between the THS group (6.3 ± 3.6 SD nmol/mg) and clean air group (2.9 ± 0.9 SD nmol/mg) (p = 0.004, mixed effects model) and 22 h between the THS group (5.9 ± 2.5 SD nmol/mg) and clean air group (3.2 ± 1.9 SD nmol/mg) (p = 0.007, mixed effects model) (Figure 2C).

Urinary biomarker of exposure

Cotinine. All THS participants had elevated urinary cotinine at 8 h (p = 0.01, paired t-test), first morning collection (p = 0.05, paired t-test), and 22 h (p = 0.04, paired t-test), indicative of nicotine exposure (See Supplementary 1 Figure 3).

Gene ontology

Proteins with ≥1.5-fold log change in expression from the THS 3 and 22-h comparison were analysed by GO which identified 13 biological processes in the 3-h group and 15 biological processes in the 22-h group that could be affected by THS exposure (Figure 3A, B). In the THS 3-h group, significant biological processes included "actin polymerization or depolymerization", "platelet aggregation", "IL-12 mediated signaling", "homotypic cell-cell adhesion", and "positive regulation of ROS metabolic process" (Figure 3A). In the THS 22-h exposure, biological processes included "endothelial cell development", "opsonization", "epithelial cell maintenance", "protein localization to the endosome", "membrane to membrane docking", "leukocyte aggregation" and "leukocyte cell-cell adhesion" (Figure 3B).

IPA networks and associated diseases or functions

The top IPA-scored network from the THS 3-h exposure was "cell-to-cell signaling and interaction, cellular function and maintenance, and infectious disease pathways" (Figure 3C). Extracellular signal-regulated kinase 1/2 (ERK1/2) was predicted to be central to these signaling pathways. Some diseases and functions associated with the THS 3-h network were inflammatory response, engulfment and phagocytosis of myeloid cells and phagocytes, engulfment of blood cells, and atherosclerosis formation. (Figure 3E). The top IPA scored network from the THS 22-h exposure was related to organismal injury and abnormalities, inflammatory response, and infectious disease. Heat shock protein 90 (Hsp90) was central to signaling proteins in this network. Diseases associated with this network were "inflammation of organs", "keratinization of epidermis", "plaque psoriasis", "dermatitis", and "exanthem of skin" (Figure 3F).

IPA regulator effect networks

IPA identified two regulator effect networks in the THS 3-h data. The first was composed of three upstream regulators (TP63, BRD4, or VIPAS39) that predictively activated seven proteins (Figure 4A). This activation may increase adhesion of cells, cell movement of leukocytes, hemostasis, activation of cells, and homing of cells (Figure 4A). The other regulator effect network predicted SMARCA4 to activate five proteins that cause proliferation of immune cells (Figure 4B). There were no other regulator networks discovered for the other exposures.

Canonical pathway analysis using IPA

Baseline, clean air 3 and 22-h pathways. The baseline comparison was performed to identify protein baseline differences between the clean air and THS data, and only one significant canonical pathway was identified, indicating that the biological changes were caused by THS exposure (Table 1). The clean air exposures were performed as a control, but also to determine the potential effects of exercise. In the clean air 22-h exposure "metabolism of reactive oxygen species" was elevated affirming exercise-induced ROS[20]; however, because no urinary biomarkers of oxidation in the control group were elevated, this suggests that there was a homeostatic redox rate. Any further ROS damage was due to THS exposure. Also, no plasma inflammatory biomarkers were found to be elevated in the clean air exposure (See Supplementary 1 Figure 4).

THS 3 and 22-h canonical pathways. The canonical pathway analysis revealed some similarities in the changes caused by THS exposure at 3 and 22 h. In the baseline to THS 3-h comparison, IPA identified ten

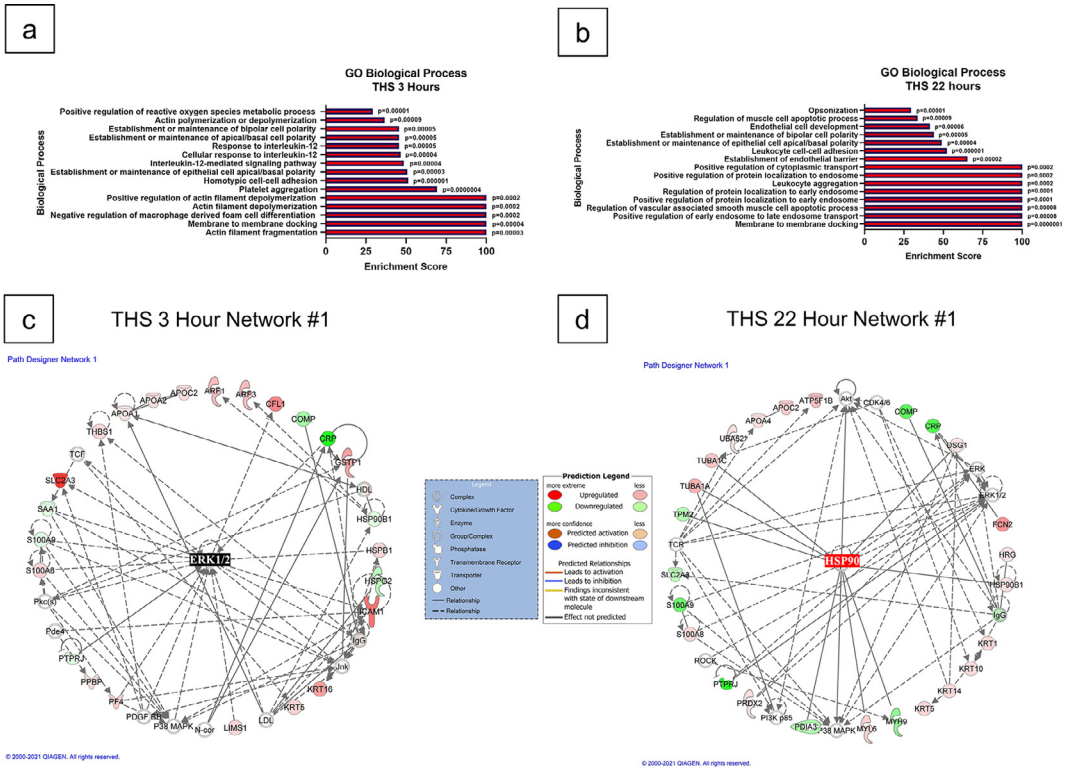

e

THS 3 hours Network #1 Diseases or Functions Association	p-value	Molecules	# Molecules
Endocytosis	2.51E-10	APOA1,APOA2,APOC2,ARF1,CRP,GSTP1,HSP90B1,HSPG2,ICAM1,IgG,LDL,P38 MAPK,PF4,Pkc(s),S100A9,SAA1,THBS1	17
Engulfment of phagocytes	2.71E-10	APOA1,APOA2,CRP,GSTP1,ICAM1,IgG,PF4,S100A9,SAA1,THBS1	10
Severe COVID-19	3.15E-10	APOA1,APOA2,CRP,PF4,PPBP,S100A8,S100A9,SAA1	8
Engulfment of leukocytes	4.92E-10	APOA1,APOA2,CRP,GSTP1,ICAM1,IgG,PF4,Pkc(s),S100A9,SAA1,THBS1	11
Phagocytosis of myeloid cells	2.52E-09	APOA1,APOA2,CRP,ICAM1,IgG,PF4,S100A9,SAA1,THBS1	9
Phagocytosis of phagocytes	2.71E-09	APOA1,APOA2,CRP,ICAM1,IgG,PF4,S100A9,SAA1,THBS1	9
Atherosclerosis	2.78E-09	APOA1,APOA2,APOC2,CRP,HDL,HSPG2,ICAM1,IgG,LDL,P38 MAPK,PDGF BB,PF4,S100A8,S100A9,SAA1,THBS1	16
Engulfment of blood cells	4.31E-09	APOA1,APOA2,CRP,GSTP1,ICAM1,IgG,LDL,PF4,Pkc(s),S100A9,SAA1,THBS1	12
Lichen planus	1.77E-08	CFL1,COMP,KRT16,KRT5,S100A8,S100A9	6
Internalization of cells	2.12E-08	APOA1,APOA2,CRP,GSTP1,ICAM1,IgG,Jnk,LDL,P38 MAPK,PF4,S100A9,SAA1,THBS1	13
Inflammatory response	2.18E-08	APOA1,CRP,ERK1/2,HDL,HSPB1,HSPG2,ICAM1,IgG,Jnk,KRT16,LDL,P38 MAPK,PF4,Pkc(s),PPBP,PTPRJ,S100A8,S100A9,SAA1,THBS1	20
Adhesion of blood cells	2.23E-08	APOA1,CRP,ERK1/2,HSPG2,ICAM1,IgG,Jnk,LDL,P38 MAPK,PF4,Pkc(s),PPBP,S100A8,S100A9,SAA1,THBS1	16

f

THS 22 hours Network #1 Diseases or Functions Association	p-value	Molecules	# Molecules
Severe COVID-19	1.65E-08	CRP,FCN2,HRG,S100A8,S100A9,TUBA1A,TUBA1C	7
Inflammation of organ	3.09E-08	Akt,APOA4,CRP,DSG1,ERK,FCN2,HSP90B1,IgG,KRT1,KRT10,KRT14,KRT5,MYH9,P38 MAPK,PDIA3,PI3K, p85,PRDX2,S100A8,S100A9,TCR,TUBA1A,TUBA1C	22
Keratinization of epidermis	4.00E-07	DSG1,KRT1,KRT10,KRT14,KRT5	5
Plaque psoriasis	5.31E-07	CRP,IgG,KRT1,KRT10,KRT14,S100A8,S100A9	7
Dermatitis	6.00E-07	DSG1,IgG,KRT1,KRT10,KRT14,KRT5,S100A8,S100A9,TUBA1A,TUBA1C	10
Benign lesion	6.00E-07	CRP,DSG1,ERK1/2,KRT1,KRT10,KRT14,KRT5,MYH9,MYL6,PRDX2,ROCK,S100A8,S100A9,TUBA1A,TUBA1C	15
Exanthem of skin	1.00E-06	Akt,CRP,IgG,KRT1,KRT10,KRT14,S100A8,S100A9	8

Figure 3. Gene ontology biological processes and IPA's predicted network activity at 3 and 22-h after THS exposure. a,b. Gene Ontology biological processes ranked by the gene enrichment score at THS 3 and 22 h. c,d. IPA's top predicted network activity at the THS 3 and 22-h time point. e,f. IPA's predicted diseases and functions associated with their THS 3- and 22-h network, respectively.

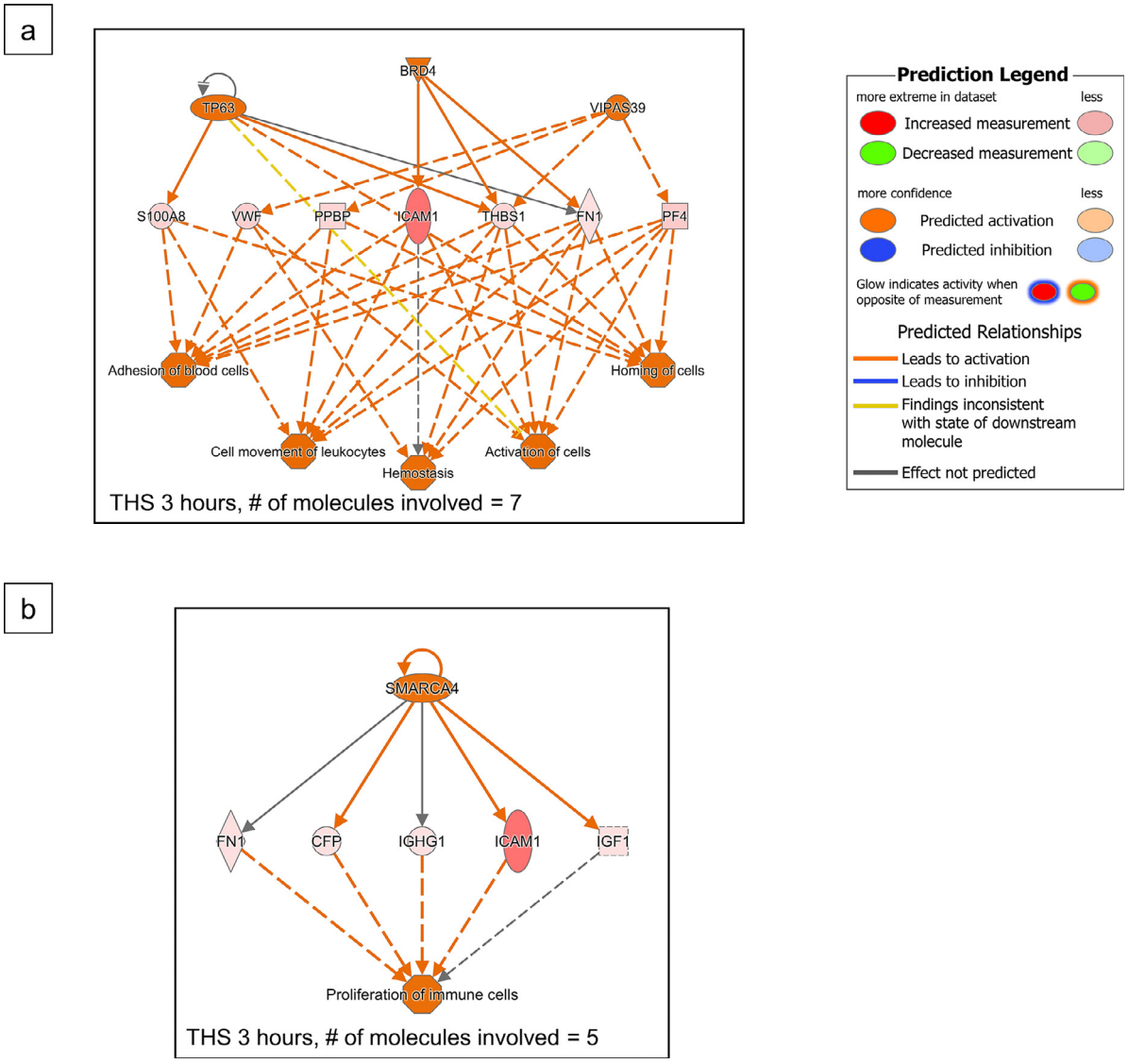

Figure 4. Upstream regulator effects predicted in the THS 3-h group by IPA. a. Predicted activation of cells, adhesion of blood cells, cell movement of leukocytes, hemostasis, and homing of cells pathways. Proteins elevated in our subjects were S100 calcium binding protein A8 (S100A8), von Willebran factor (VWF), pro-platelet binding protein (PPBP), (intracellular adhesion molecule 1) ICAM1, (thrombospondin 1) THBS1, (fibronectin 1) FN1, and (platelet factor 4) PF4 that were predicted to be regulated by (tumor protein p63) TP63, (bromodomain-containing protein 4) BRD4, or (spermatogenesis-defective protein 39 homolog) VIPAS39. b. Predicted proliferation of immune cells pathway. Proteins elevated in our subjects were FN1, (complement factor properdin) CFP, (immunoglobulin heavy constant gamma 1) IGHG1, ICAM1, and (insulin-like growth factor 1) IGF1 that were predicted to be regulated by (SWI/SNF related, matrix associated, actin dependent regulator of chromatin, subfamily A, member 4) SMARCA4.

significant canonical pathways, which included "production of nitric oxide and ROS in macrophages", "leukocyte extravasation signaling", and "cardiac hypertrophy" (Table 1). The THS 22-h group had four significant canonical pathways which correlated with our biomarker results and included production of "nitric oxide and ROS in macrophages", "leukocyte extravasation signaling", and "IL-8 signaling".

THS 3 and 22-h disease and bio functions. A "Disease and Bio Functions" analysis was performed in IPA, Fourteen "Disease and Bio Functions" were activated in the THS 3-h comparison, and these included "cell movement", "migration of cells", cell movement of leukocytes, lymphocytes, and phagocytes, "adhesion of blood cells", and "hemostasis". IPA predicted nine Bio Functions for the THS 22-h group, which included "cell

Timepoint	Canonical pathways	Z-score	Predicated activation state
Baseline (clean air 0 h vs THS 0 h)			
	Huntington's Disease Signaling	-2	Decreased
Clean Air 3 h (clean air 0 h vs clean air 22 h)			
	RhoGDI Signaling	2	Increased
	Huntington's Disease Signaling	-2.236	Decreased
	Integrin Signaling	-2.236	Decreased
	Actin Cytoskeleton Signaling	-2.449	Decreased
Clean Air 22 h (clean air 0 h vs clean air 22 h)			
	Fcγ Receptor-mediated Phagocytosis in Macrophages and Monocytes	-2	Decreased
	Xenobiotic Metabolism PXR Signaling Pathway	-2	Decreased
	Huntington's Disease Signaling	-2.236	Decreased
THS 3 h (THS 0 h vs THS 3 h)			
	Leukocyte Extravasation Signaling	2.828	Increased
	RhoA Signaling	2.714	Increased
	Actin Cytoskeleton Signaling	2.673	Increased
	Paxillin Signaling	2.449	Increased
	Signaling by Rho Family GTPases	2.333	Increased
	Coronavirus Replication Pathway	2.236	Increased
	Tumor Microenvironment Pathway	2.236	Increased
	Production of Nitric Oxide and Reactive Oxygen Species in Macrophages	2.121	Increased
	Cardiac Hypertrophy Signaling	2	Increased
	Phospholipase C Signaling	2	Increased
THS 22 h (THS 0 h vs THS 22 h)			
	Production of Nitric Oxide and Reactive Oxygen Species in Macrophages	2.646	Increased
	Huntington's Disease Signaling	2	Increased
	MSP-RON Signaling In Cancer Cells Pathway	2	Increased
	IL-8 Signaling	2	Increased

***Table 1*: Predicted significant IPA canonical pathways for each comparison group.**

movement", "migration of cells", "cell spreading of tumor cell lines", "cell movement of phagocytes", "vasculogenesis", and "angiogenesis" (Table 2).

Western blot for integrin-linked kinase (ILK) and beta-3 integrin

To validate the proteomics data, Western blots were performed on plasma from the subjects used in the proteomics study. There were similar increases in ILK and beta-3 integrin expression at the 3- and 22-h THS exposures and no change in the clean air exposure (See Supplementary 1 Figures 5, 6).

Discussion

This proof-of-concept human clinical study identified molecular pathways and potential health risks associated with dermal exposure to THS, which is likely the main route of uptake of THS chemicals from the environment. Acute THS exposure caused elevation of urinary biomarkers of oxidative damage to DNA, lipids, and proteins, and biomarkers remained high after exposure stopped. Cotinine, a nicotine metabolite, was significantly elevated in the urine of THS subjects after 8 h, verifying systemic organ exposure to THS chemicals. Proteomics analysis detected differences between the THS and clean air exposures consistent with oxidative damage caused by THS toxicants, and implicated activation of the pro-inflammatory innate immune system, which initiated molecular risk factors for inflammatory skin disease.

Cigarette smoking increases inflammation,[21] recruits leukocytes to injured tissue,[22] and stimulates a pro-inflammatory immune response.[23] Smoking is also a risk factor for thrombosis-induced stroke because it elevates red blood cell counts[24] and forms sticky fibrin clots.[25] Like cigarette smoking, THS exposure activated functional pathways characteristic of an innate immune response (e.g., "inflammatory response", "inflammation

Timepoint	Disease and biological functions	Z-score	Predicated activation state
Baseline (clear air 0 h vs THS 0 h)	Binding of mononuclear leukocytes	1.964	Increased
	Lymphocyte migration	1.962	Increased
	Proliferation of cancer cells	-1.964	Decreased
	Viral Infection	-2.025	Decreased
	Vasculogenesis	-2.157	Decreased
	Growth of connective tissue	-2.204	Decreased
Clean Air 3 h (clean air 0 h vs clean air 3 h)			
	Survival of vascular cells	-2	Decreased
	Formation of actin stress fibers	-2.2	Decreased
	Survival of sarcoma cell lines	-2.201	Decreased
Clean Air 22 h (clean air 0 h vs clean air 22 h)			
	Migration of granulocytes	2.207	Increased
	Metabolism of reactive oxygen species	2.02	Increased
	Apoptosis of endothelial cell lines	-1.98	Decreased
	Formation of actin filaments	-2.207	Decreased
	Formation of filaments	-2.207	Decreased
	Chemotaxis of phagocytes	-2.23	Decreased
THS 3 h (THS 0 h vs THS 3 h)			
	Cell movement	2.892	Increased
	Activation of cells	2.701	Increased
	Cell movement of leukocytes	2.684	Increased
	Migration of cells	2.631	Increased
	Leukocyte migration	2.618	Increased
	Cell movement of mononuclear leukocytes	2.615	Increased
	Adhesion of blood cells	2.471	Increased
	Cell movement of lymphocytes	2.233	Increased
	Organization of cytoplasm	2.231	Increased
	Organization of cytoskeleton	2.231	Increased
	Hemostasis	2.203	Increased
	Homing of cells	2.093	Increased
	Proliferation of immune cells	2.088	Increased
	Proliferation of mononuclear leukocytes	2.088	Increased
	Cell spreading	2.068	Increased
	Chemotaxis	2.059	Increased
	Adhesion of immune cells	2.001	Increased
THS 22 h (THS 0 h vs THS 22 h)			
	Vasculogenesis	3.087	Increased
	Cell spreading	2.795	Increased
	Cell movement	2.759	Increased
	Cell spreading of tumor cell lines	2.646	Increased
	Angiogenesis	2.45	Increased
	Migration of cells	2.342	Increased
	Proliferation of blood cells	2.155	Increased
	Cell movement of phagocytes	2.135	Increased
	Activation of cells	2.046	Increased

***Table 2*: Predicted significant IPA disease and biological functions for each comparison group.**

of organ", "leukocyte migration", "proliferation of immune cells", and "phagocytosis by myeloid cells"). IPA predicted two upstream regulatory pathways from the THS 3-h exposure, which included "elevated hemostasis", "adhesion of blood cells", "cell activation", "movement of leukocytes and homing of cells" and "increased proliferation of immune cells". IL-6, a pro-inflammatory cytokine, was significantly higher after 3-h exposure to THS and remained elevated at 22 h. Similar increases in inflammatory cytokines occurred in a 3D model of human epidermis (EpiDerm) exposed to the residue from exhaled electronic cigarette aerosol.[26] Furthermore, the top scored biofunctions network were "inflammatory response" at 3 h and "inflammation of

organs" at 22 h. Together, our results demonstrate that exposure to THS increases hemostasis ("adhesion of blood cells") and initiates a pro-inflammatory response, which are risk factors for thrombosis.

Upregulation of "RhoA signaling" and "signaling of Rho family GTPases" in the 3-h THS exposure group provides further evidence for activation of the innate immune system. RhoA, a member of the RhoA GTPase family, regulates actin cytoskeletal organization,[27] NF-κB transactivation,[28] and IL-8 synthesis in endothelial cells.[29] Exposure of human epithelial cells to cigarette smoke extract for 3 h activated a RhoA-dependent NF-κB signaling pathway that stimulated pro-inflammatory cytokine production.[30] Similarly, the 3-h THS exposure increased RhoA signaling, which activated "actin cytoskeleton signaling" and pro-inflammatory cytokine "IL-8 signaling" the next day. Macrophages produces large amounts of ROS from their "oxidative burst"[31] and similarly in both THS exposures "production of nitric oxide and reactive oxygen species in macrophages" were elevated. The pro-immune system is likely to contribute to the elevation of urinary biomarkers of oxidative harm in the THS exposure. These results support the idea that THS exposure mimics the oxidative damage and immune activation previously observed in cigarette smokers.[21,23,32]

Our THS exposures were brief, did not cause skin irritation, and were unlikely to induce skin disease, nevertheless markers associated with early-stage activation of contact dermatitis, psoriasis and other skin conditions were elevated. Allergic contact dermatitis is a rash caused by an immune reaction to materials that touch the skin,[33] and psoriasis is characterised by cutaneous plaques caused by inflammatory infiltrates and epidermal hyperproliferation.[34] Psoriasis is linked to genetic susceptibility and can be triggered by environmental factors.[35] These skin diseases have been linked to cigarette usage[34,36] and markers of both diseases were elevated in the plasma from subjects exposed to THS. At 22-h after THS exposure, the proteomics data showed higher concentrations of markers associated with "keratinization of the epidermis", "plaque psoriasis", "dermatitis", and "exanthem of the skin". Concentrations of keratin 5 (KRT5) and keratin 14 (KRT14), the major cytokeratins of the epidermis, were elevated 22-h after THS exposure. Repeated cigarette exposure to epithelial cells produced similar increases in KRT5 and KRT14,[37] which are biomarkers linked to inflammation-driven skin diseases, such as dermatitis and psoriasis.[38,39] While our subjects did not develop these conditions during their 3-h exposure to THS, molecular changes characteristic of skin irritation and inflammation occurred, supporting the idea that dermal exposure to THS could lead to molecular initiation of inflammation-induced skin diseases.

Chronic exposure to THS may cause other diseases. Unrepaired DNA damage increases the risk of developing cancer.[40] "Positive regulation of reactive oxygen metabolic processes" was upregulated at THS 3-h exposure. 8-isoprostane, indicative of lipid oxidation, is associated with atherosclerosis, cardiac failure, cancer, and immunological disorders.[41] Protein oxidation causes protein fragmentation and protein-protein cross-linking, which impair function, potentially leading to diseases such as chronic obstructive pulmonary disease (COPD).[42]

Cigarette smoke-induced atherosclerosis includes activation of a pro-inflammatory system and remodeled vasculature.[43,44,45] Macrophages phagocytose and clear oxidized lipids and become foam cells, preventing lipid clots.[45] In cigarette smokers, vascular smooth muscle cells (SMCs) increase matrix remodeling and inflammatory gene expression.[46] The activation of MMPs causes vascular SMC apoptosis leading to a loss of vascular structural integrity.[47] Our THS-exposed subjects showed activation of atherosclerosis and similar atherogenesis-related pathways. IPA predicted "negative regulation of macrophage derived foam cell differentiation" that would reduce clearance of lipids, leading to accumulation of oxidized lipids in blood vessels. The "regulation of vascular associated SMC apoptotic process" and elevation of inflammation pathways mimic atherogenesis. The "adhesion of blood cells" pathway could lead to platelet aggregation. Our data suggest that prolonged THS exposure could produce arterial plaques and atherosclerosis, as seen in cigarette smokers.

We explored the predicted molecular proteins that regulated the biological pathways affected in our subjects. THS exposure activated biological functions associated with increased cell migratory and survival pathways, such as "cell movement", "cell spreading of tumor lines", "migration of cells", "vasculogenesis", and "angiogenesis". The highest scored IPA THS 3-h network was "cell-to-cell signaling and interaction, cellular function and maintenance, and infectious disease pathways". ERK1/2, a protein-serine/threonine kinase, was predicted as a central signaling molecule in this network. ERK1/2 signals in pathways that regulate cell migration, cell survival, cell cycle progression, differentiation, and proliferation.[48] Nicotine binds to nAChR and β-adrenoceptors resulting in a downstream cascade of ERK/1/2/Stat3-signaling, which in turn activates NF-κB transcription of the cell-cycle regulator cyclin D1, a promoter of cell proliferation.[49] The THS 22-h exposure's highest scored IPA network was "organismal injury and abnormalities, inflammatory response, and infectious disease" pathways. HSP90, which acts as a chaperone for ERK1/2,[50] was central to interacting with the majority of proteins in this network. We predict HSP90 was induced as a survival response to help cells maintain protein homeostasis and DNA stability in an oxidative and chemically toxic environment.

Conclusions

Our study demonstrates that acute dermal exposure to THS increased oxidation of urinary DNA, lipids, and

proteins and produced changes in the plasma proteome that are similar to those observed in cigarette smokers. THS exposure activated the innate immune system, increased oxidative stress, and elevated biomarkers associated with skin diseases, such as contact dermatitis and psoriasis. Pathways associated with other cigarette-induced diseases not involving the skin, such as atherosclerosis and cancer, were also elevated in THS-exposed subjects. Though the subjects did not develop these diseases during a 3-h exposure to THS, our results provide molecular evidence that proteins involved in disease pathways were elevated in a subset of humans after acute dermal exposure to THS. Our data, which contribute to the growing literature on THS,[51] will be useful in devising regulatory policies to limit exposure to THS in contaminated properties and will enable healthcare workers to advise their patients on the risks associated with THS exposure. Electronic cigarettes also deposit a residue that comes into contact with the skin,[26,52,53] and this should be evaluated in future studies. The evaluation of larger populations exposed for longer periods of exposure would further characterise human health responses to dermal THS exposure.

Contributors

Dr. Sakamaki-Ching and Dr. Talbot had full access to all of the data in the study and take responsibility for the integrity of the data and the accuracy of the data analysis. All authors have read and approved the manuscript.
Concept and design: All authors.
Acquisition, analysis, or interpretation of data: All authors.
Drafting of the manuscript: Sakamaki-Ching, Talbot.
Critical revision of the manuscript for important intellectual content: All authors.
Statistical analysis: Sakamaki-Ching, Li.
Obtained funding: Schick, Talbot.
Administrative, technical, or material support: All authors
Supervision: Schick, Talbot.

Data sharing statement

Participant information can be made available by contacting Dr. Schick by email.

Declaration of interests

The authors did not receive direct funding for this project. Funding from TRDRP was administered via the institution. All authors declare no direct support from any organization for the submitted work, no financial relationships with any organizations that might have an interest in the submitted work in the previous three years, and no other relationships or activities that could appear to have influenced the submitted work.

Acknowledgements

Dr. Brett Phinney made contributions to the study. He is employed by the University of California, Davis Proteomics Core Facility. Funding was provided by the Tobacco Related Disease Research Program (TRDRP) 24RT-0037 TRDRP, 24RT-0039 TRDRP, and 28PT-0081 TRDRP.

Supplementary materials

Supplementary material associated with this article can be found in the online version at doi:10.1016/j.ebiom.2022.104256.

References

1 Matt GE, Quintana PJE, Destaillats H, et al. Thirdhand tobacco smoke: emerging evidence and arguments for a multidisciplinary research agenda. *Environ Health Perspect*. 2011;119(9):1218–1226. https://doi.org/10.1289/ehp.1103500.
2 Destaillats H, Singer BC, Lee SK, Gundel LA. Effect of ozone on nicotine desorption from model surfaces: evidence for heterogeneous chemistry. *Environ Sci Technol*. 2006;40(6):1799–1805. https://doi.org/10.1021/es0509014r.
3 Sleiman M, Gundel LA, Pankow JF, Jacob P, Singer BC, Destaillats H. Formation of carcinogens indoors by surface-mediated reactions of nicotine with nitrous acid, leading to potential thirdhand smoke hazards. *PNAS*. 2010;107(15):6576–6581. https://doi.org/10.1073/pnas.0912820107.
4 Bahl V, Iii PJ, Havel C, Schick SF, Talbot P. Thirdhand cigarette smoke: factors affecting exposure and remediation. *PLoS One*. 2014;9(10):e108258. https://doi.org/10.1371/journal.pone.0108258.
5 Jacob P, Benowitz NL, Destaillats H, et al. Thirdhand smoke: new evidence, challenges, and future directions. *Chem Res Toxicol*. 2017;30(1):270–294. https://doi.org/10.1021/acs.chemrestox.6b00343.
6 Bahl V, Johnson K, Phandthong R, Zahedi A, Schick SF, Talbot P. From the cover: thirdhand cigarette smoke causes stress-induced mitochondrial hyperfusion and alters the transcriptional profile of stem cells. *Toxicol Sci*. 2016;153(1):55–69. https://doi.org/10.1093/toxsci/kfw102.
7 Bahl V, Weng NJH, Schick SF, et al. Cytotoxicity of thirdhand smoke and identification of acrolein as a volatile thirdhand smoke chemical that inhibits cell proliferation. *Toxicol Sci*. 2016;150(1):234–246. https://doi.org/10.1093/toxsci/kfv327.
8 Hang B, Sarker AH, Havel C, et al. Thirdhand smoke causes DNA damage in human cells. *Mutagenesis*. 2013;28(4):381–391. https://doi.org/10.1093/mutage/get013.
9 Xu B, Chen M, Yao M, et al. Metabolomics reveals metabolic changes in male reproductive cells exposed to thirdhand smoke. *Sci Rep*. 2015;5(1):15512. https://doi.org/10.1038/srep15512.
10 Martins-Green M, Adhami N, Frankos M, et al. Cigarette smoke toxins deposited on surfaces: implications for human health. Sun Q, ed. *PLoS One*. 2014;9(1):e86391. https://doi.org/10.1371/journal.pone.0086391.
11 Karim ZA, Alshbool FZ, Vemana HP, et al. Third-hand smoke: impact on hemostasis and thrombogenesis. *J Cardio Pharma*. 2015;66(2):177–182. https://doi.org/10.1097/FJC.0000000000000260.
12 Hang B, Wang Y, Huang Y, et al. Short-term early exposure to thirdhand cigarette smoke increases lung cancer incidence in mice. *Clin Sci*. 2018;132(4):475–488. https://doi.org/10.1042/CS20171521.
13 Torres S, Samino S, Ràfols P, Martins-Green M, Correig X, Ramírez N. Unravelling the metabolic alterations of liver damage induced by thirdhand smoke. *Environ Int*. 2021;146:106242. https://doi.org/10.1016/j.envint.2020.106242.
14 Ramírez N, Özel MZ, Lewis AC, Marcé RM, Borrull F, Hamilton JF. Exposure to nitrosamines in thirdhand tobacco smoke increases cancer risk in non-smokers. *Environ Int*. 2014;71:139–147. https://doi.org/10.1016/j.envint.2014.06.012.
15 Pozuelos GL, Kagda MS, Schick S, Girke T, Volz DC, Talbot P. Experimental acute exposure to thirdhand smoke and changes in the human nasal epithelial transcriptome: a randomized clinical trial. *JAMA Netw Open*. 2019;2(6):e196362. https://doi.org/10.1001/jamanetworkopen.2019.6362.
16 Schick SF, Farraro KF, Fang J, et al. An apparatus for generating aged cigarette smoke for controlled human exposure studies. *Aerosol Sci and Tech*. 2012;46(11):1246–1255. https://doi.org/10.1080/02786826.2012.708947.
17 Frey PF, Ganz P, Hsue PY, et al. The exposure-dependent effects of aged secondhand smoke on endothelial function. *J Am Coll Cardiol*. 2012;59:1908–1913. https://doi.org/10.1016/j.jacc.2012.02.025.

18 Heiss C, Amabile N, Lee AC, et al. Brief secondhand smoke exposure depresses endothelial progenitor cells activity and endothelial function: sustained vascular injury and blunted nitric oxide production. *J Am Coll Cardiol*. 2008;51:1760–1771. https://doi.org/10.1016/j.jacc.2008.01.040.

19 Rice SJ, Liu X, Miller B, et al. Proteomic profiling of human plasma identifies apolipoprotein E as being associated with smoking and a marker for squamous metaplasia of the lung. *Proteomics*. 2015;15(18):3267–3277. https://doi.org/10.1002/pmic.201500029.

20 Powers SK, Deminice R, Ozdemir M, Yoshihara T, Bomkamp MP, Hyatt H. Exercise-induced oxidative stress: friend or foe? *J Sport Health Sci*. 2020;9(5):415–425. https://doi.org/10.1016/j.jshs.2020.04.001.

21 Lee J, Taneja V, Vassallo R. Cigarette smoking and inflammation. *J Dent Res*. 2012;91(2):142–149. https://doi.org/10.1177/0022034511421200.

22 Scott D, Palmer R. The influence of tobacco smoking on adhesion molecule profiles. *Tob Induc Dis*. 2002;1(1):7–25. https://doi.org/10.1186/1617-9625-1-1-7.

23 Qiu F, Liang CL, Liu H, et al. Impacts of cigarette smoking on immune responsiveness: up and down or upside down? *Oncotarget*. 2016;8(1):268–284. https://doi.org/10.18632/oncotarget.13613.

24 Pedersen KM, Çolak Y, Ellervik C, Hasselbalch HC, Bojesen SE, Nordestgaard BG. Smoking and increased white and red blood cells. *Arterioscl, Thromb, Vascul Biol*. 2019;39(5):965–977. https://doi.org/10.1161/ATVBAHA.118.312338.

25 Pretorius E, Oberholzer HM, der Spuy WJ van, Meiring JH. Smoking and coagulation: the sticky fibrin phenomenon. *Ultrastructural Pathol*. 2010;34(4):236–239. https://doi.org/10.3109/01913121003743716.

26 Khachatoorian C, Luo W, McWhirter KJ, Pankow JF, Talbot P. E-cigarette fluids and aerosol residues cause oxidative stress and an inflammatory response in human keratinocytes and 3D skin models. *Toxicol In Vitro*. 2021;77:105234. https://doi.org/10.1016/j.tiv.2021.105234.

27 Sit ST, Manser E. Rho GTPases and their role in organizing the actin cytoskeleton. *J Cell Sci*. 2011;124(5):679–683. https://doi.org/10.1242/jcs.064964.

28 Perona R, Montaner S, Saniger L, Sánchez-Pérez I, Bravo R, Lacal JC. Activation of the nuclear factor-kappaB by Rho, CDC42, and Rac-1 proteins. *Genes Dev*. 1997;11(4):463–475. https://doi.org/10.1101/gad.11.4.463.

29 Guo F, Tang J, Zhou Z, et al. GEF-H1-RhoA signaling pathway mediates LPS-induced NF-κB transactivation and IL-8 synthesis in endothelial cells. *Mol Immunol*. 2012;50(1-2):98–107. https://doi.org/10.1016/j.molimm.2011.12.009.

30 Zhang C, Qin S, Qin L, et al. Cigarette smoke extract-induced p120-mediated NF-κB activation in human epithelial cells is dependent on the RhoA/ROCK pathway. *Sci Rep*. 2016;6(23131):1–12. https://doi.org/10.1038/srep23131.

31 Yang Y, Bazhin AV, Werner J, Karakhanova S. Reactive oxygen species in the immune system. *Int Rev Immunol*. 2013;32(3):249–270. https://doi.org/10.3109/08830185.2012.755176.

32 Zuo L, He F, Sergakis GG, et al. Interrelated role of cigarette smoking, oxidative stress, and immune response in COPD and corresponding treatments. *Am J Physiol-Lung Cell Mol Physiol*. 2014;307(3):L205–L218. https://doi.org/10.1152/ajplung.00330.2013.

33 Adler BL, DeLeo VA. Allergic contact dermatitis. *JAMA Dermatol*. 2021;157(3):364. https://doi.org/10.1001/jamadermatol.2020.5639.

34 Fortes C, Mastroeni S, Leffondré K, et al. Relationship between smoking and the clinical severity of psoriasis. *Arch Dermatol*. 2005;141(12):1580–1584. https://doi.org/10.1001/archderm.141.12.1580.

35 Zeng J, Luo S, Huang Y, Lu Q. Critical role of environmental factors in the pathogenesis of psoriasis. *J Dermatol*. 2017;44(8):863–872. https://doi.org/10.1111/1346-8138.13806.

36 Kim SY, Sim S, Choi HG. Atopic dermatitis is associated with active and passive cigarette smoking in adolescents. *PLoS One*. 2017;12(11):e0187453. https://doi.org/10.1371/journal.pone.0187453.

37 Schamberger AC, Staab-Weijnitz CA, Mise-Racek N, Eickelberg O. Cigarette smoke alters primary human bronchial epithelial cell differentiation at the air-liquid interface. *Sci Rep*. 2015;5(8163):1–8. https://doi.org/10.1038/srep08163.

38 Wei X, Fricker K, Enk AH, Hadaschik EN. Altered expression of keratin 14 in lesional epidermis of autoimmune skin diseases. *Int J Dermatol*. 2016;55(6):620–628. https://doi.org/10.1111/ijd.13011.

39 Leung DYM, Calatroni A, Zaramela LS, et al. The nonlesional skin surface distinguishes atopic dermatitis with food allergy as a unique endotype. *Sci Transl Med*. 2019;11(480):eaav2685. https://doi.org/10.1126/scitranslmed.aav2685.

40 Loft S, Poulsen HE. Cancer risk and oxidative DNA damage in man. *J Mol Med*. 1996;74(6):297–312. https://doi.org/10.1007/BF00207507.

41 Ramana KV, Srivastava S, Singhal SS. Lipid peroxidation products in human health and disease. *Oxid Med Cell Longev*. 2013;2013:583438. https://doi.org/10.1155/2013/583438.

42 Davies MJ. Protein oxidation and peroxidation. *Biochem J*. 2016;473(Pt 7):805–825. https://doi.org/10.1042/BJ20151227.

43 Ambrose John A, Barua Rajat S. The pathophysiology of cigarette smoking and cardiovascular disease. *J Am Coll Cardiol*. 2004;43(10):1731–1737. https://doi.org/10.1016/j.jacc.2003.12.047.

44 Perlstein Todd S, Lee Richard T. Smoking, metalloproteinases, and vascular disease. *Arterioscl, Thromb, Vascul Biol*. 2006;26(2):250–256. https://doi.org/10.1161/01.ATV.0000199268.27395.4f.

45 Messner B, Bernhard D. Smoking and cardiovascular disease. *Arterioscl, Thromb, Vascul Biol*. 2014;34(3):509–515. https://doi.org/10.1161/ATVBAHA.113.300156.

46 Starke RM, Ali MS, Jabbour PM, et al. Cigarette smoke modulates vascular smooth muscle phenotype: implications for carotid and cerebrovascular disease. *PLoS One*. 2013;8(8):e71954. https://doi.org/10.1371/journal.pone.0071954.

47 Wang X, Khalil RA. Matrix metalloproteinases, vascular remodeling, and vascular disease. *Adv Pharmacol*. 2018;81:241–330. https://doi.org/10.1016/bs.apha.2017.08.002.

48 Roskoski R. ERK1/2 MAP kinases: structure, function, and regulation. *Pharmacol Res*. 2012;66(2):105–143. https://doi.org/10.1016/j.phrs.2012.04.005.

49 Chen RJ, Ho YS, Guo HR, Wang YJ. Rapid activation of Stat3 and ERK1/2 by nicotine modulates cell proliferation in human bladder cancer cells. *Toxicol Sci*. 2008;104(2):283–293. https://doi.org/10.1093/toxsci/kfn086.

50 Liu D, Yuan H, Cao C, et al. Heat shock protein 90 acts as a molecular chaperone in late-phase activation of extracellular signal-regulated kinase 1/2 stimulated by oxidative stress in vascular smooth muscle cells. *Acta Pharmacol Sin*. 2007;28(12):1907–1913. https://doi.org/10.1111/j.1745-7254.2007.00702.x.

51 Díez-Izquierdo A, Cassanello-Peñarroya P, Lidón-Moyano C, Matilla-Santander N, Balaguer A, Martínez-Sánchez JM. Update on thirdhand smoke: a comprehensive systematic review. *Environ Res*. 2018;167:341–371. https://doi.org/10.1016/j.envres.2018.07.020.

52 Khachatoorian C, Jacob P, Sen A, Zhu Y, Benowitz NL, Talbot P. Identification and quantification of electronic cigarette exhaled aerosol residue chemicals in field sites. *Environ Res*. 2019;170:351–358. https://doi.org/10.1016/j.envres.2018.12.027.

53 Khachatoorian C, Jacob P, Benowitz NL, Talbot P. Electronic cigarette chemicals transfer from a vape shop to a nearby business in a multiple-tenant retail building. *Tob Control*. 2019;28(5):519–525. https://doi.org/10.1136/tobaccocontrol-2018-054316.